Supporting information:

High thermoelectric performance in n-type BiAgSeS due to intrinsically low thermal conductivity†

Yan-Ling Pei,[a,⊥] Haijun Wu,[b,⊥] Jiehe Sui,[c,⊥] Jing Li,[c] David Berardan,[d] Celine Barreteau,[d] Lin Pan,[d] Nita Dragoe,[d] Wei-Shu Liu,[e] Jiaqing He,[b,*] Li-Dong Zhao,[d,*]

[a]*School of Materials Science and Engineering, Beihang University, Beijing 100191, China*
[b]*Department of Physics, South University of Science and Technology of China, Shenzhen 518055, P. R. China*
E-mail: he.jq@sustc.edu.cn
[c]*National Key Laboratory Precision Hot Processing of Metals, School of Materials Science and Engineering, Harbin Institute of Technology, Harbin 150001, China*
[d]*LEMHE, ICMMO, University Paris-Sud & CNRS, Orsay F-91405, France*
(L.-D. Zhao is presently in Department of Chemistry, Northwestern University, Evanston, Illinois 60208, USA.)
E-mail: lidong-zhao@northwestern.edu
[e]*Department of Physics, Boston College, Chestnut Hill, Massachusetts 02467, USA*

[⊥]*Y.-L. Pei, H. Wu and J. Sui contributed equally to this work.*

Part 1, Experimental details and characterizations:

Synthesis: Samples with the chemical composition $BiAgSeS_{1-x}Cl_x$, (x = 0, 0.01, 0.02, 0.03, 0.04 and 0.05) were synthesized by mixing appreciated ratios of high purity starting materials of Bi, Ag, Se, S and $BiCl_3$ in quartz tubes under an N_2-filled glove box. The tubes were then evacuated to a pressure of ~10^{-4} torr, flame-sealed, slowly heated to 723 K in 12 h, then to 1123 K in 4 h, soaked at this temperature for 6 h and subsequently water quenched to room temperature. The obtained ingots were crushed into powders, then ball milled at 250rpm for 8h in a planetary ball mill. The obtained powders were sintered by spark plasma sintering system (Sumimoto SPS1050, Japan) under the axial compressive stress of 50MPa in vacuum at 823K for 6min, resulting in high dense Ø20×7mm disk-shaped pellets. Finally, the obtained samples were sealed inside an evacuated quartz tube with a pressure of ~10^{-4} torr and annealed at 823 K for 7 days, to ensure that the samples microstructure is thermodynamically stable at the highest temperature used for the measurements.

Electrical properties: The obtained SPS processed pellets were cut along the radial direction of a disk sample into bars with dimensions about 18 mm × 3 mm × 3 mm that were used for simultaneous measurement of the Seebeck coefficient and the electrical conductivity using an Ulvac Riko ZEM-2 instrument (ZEM-2, ULVAC-RIKO, Japan) under a helium atmosphere from room temperature to 823 K. Heating and cooling cycles gave repeatable electrical properties to verify the thermal stability. Electrical properties obtained from different slices cut from the same pellets were similar, attesting to the homogeneity of the samples. The uncertainty of the Seebeck coefficient and electrical conductivity measurements is 5%. The Hall coefficients, R_H, of the samples were measured at room temperature using a physical properties measurement system (PPMS-9T, Quantum Design Inc, USA), and a magnetic field of 2T and electrical current of 30mA were applied. The carrier concentration (n_H) was calculated by n_H=1/eR_H, where e is the electronic charge. The carrier mobility (μ) was calculated by $\mu=\sigma R_H$, where σ is the electrical resistivity.

Thermal conductivity: High density SPS processed pellets were cut along the

SPS pressing direction and make the thermal and electrical transport properties were measured along the same direction in the sample. The SPS processed pellets were polished into coins of Ø ~ 6 mm and 1-2 mm thickness for thermal diffusivity measurements. The samples were coated with a thin layer of graphite to minimize errors from the emissivity of the material. The thermal conductivity was calculated from $\kappa = D \cdot C_p \cdot \rho$, where the thermal diffusivity coefficient (D) in the range room temperature to 823K was measured using the laser flash diffusivity method in a Netzsch LFA427 (NETZSCH, LFA427, Germany), the thermal diffusivity data were analyzed using a Cowan model with pulse correction and heating and cooling cycles give reproducible values for each sample. The specific heat capacity (C_p) was determined by differential scanning calorimetry (NETZSCH DSC 404C Germany). The density (ρ) was determined by using the dimensions and mass of the sample, which was then reconfirmed using the Archimedes method (Table S1). Thermal diffusivities obtained for different slices from the same pellet are also similar. The uncertainty of the thermal conductivity is estimated to be within 8%, considering the uncertainties for D, C_p and ρ. The combined uncertainty for all measurements involved in the calculation of ZT is less than 15%.

X-ray diffraction and Transmission electron microscopy: Samples pulverized in an agate mortar were used for powder X-ray diffraction, phase structure was analyzed using by X-ray diffraction (XRD, CuKα, Bruker D8, Germany). Transmission electron microscopy (TEM) investigations were carried out in a JEOL 2100F microscope. The thin TEM specimens were prepared by conventional standard methods. The procedures include cutting, grinding, dimpling, polishing and Ar-ion milling on a liquid nitrogen cooling state subsequently. Scanning electron microscopy (SEM) studies were performed using a Hitachi S-3400N VP-SEM equipped with an Oxford detector for energy dispersive X-ray spectroscopy (EDS).

Band gap measurement: Room temperature optical diffuse reflectance measurements were performed on finely ground powders to probe optical energy gap of the series. The spectra were collected by the measurements using a Shimadzu

Model UV-3101PC double-beam, double-monochromator spectrophotometer (Ultraviolet-Visible absorption Spectra). $BaSO_4$ was used as a 100% reflectance standard. The reflectance versus wavelength data generated, were used to estimate the band gap by converting reflectance to absorption data according to Kubelka-Munk equations: $\alpha/S = (1-R)^2/(2R)$, where R is the reflectance and α and S are the absorption and scattering coefficients, respectively.

Part 2, EDS analysis:

BiAgSeS

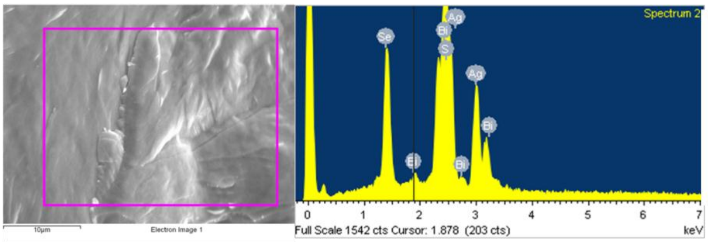

Element	Weight%	Atomic%
S K	7.35	24.69
Se L	17.41	23.74
Ag L	26.50	26.46
Bi M	48.74	25.11
Totals	100.00	

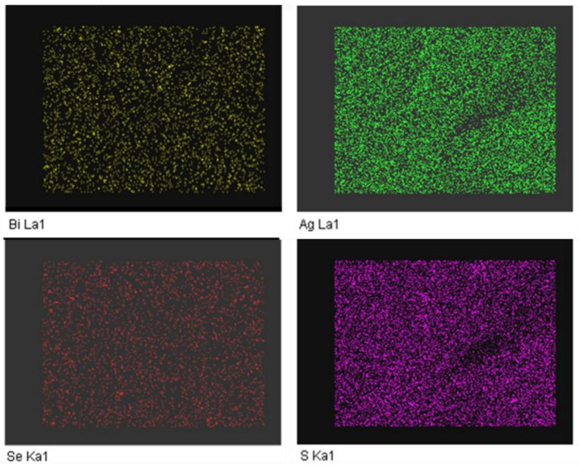

$BiAgSeS_{0.99}Cl_{0.01}$

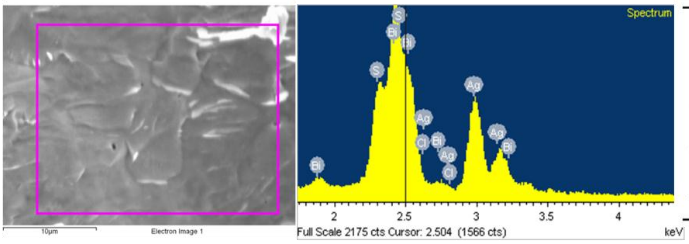

Element	Weight%	Atomic%
S K	7.29	24.20
Cl K	0.17	0.51
Se L	18.15	24.48
Ag L	27.01	26.67
Bi M	47.38	24.14
Totals	100.00	

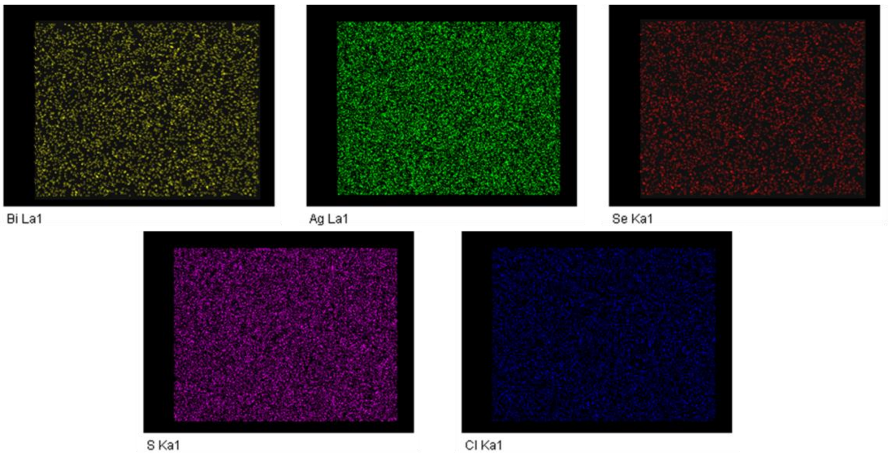

$BiAgSeS_{0.98}Cl_{0.02}$

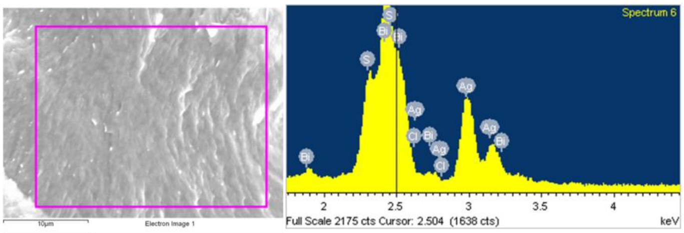

Element	Weight%	Atomic%
S K	7.48	25.01
Cl K	0.18	0.54
Se L	17.60	23.87
Ag L	25.55	25.37
Bi M	49.19	25.22
Totals	100.00	

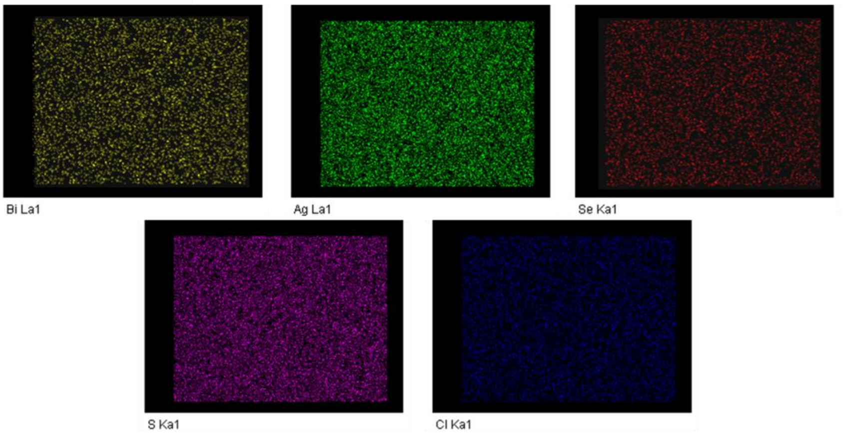

$BiAgSeS_{0.97}Cl_{0.03}$

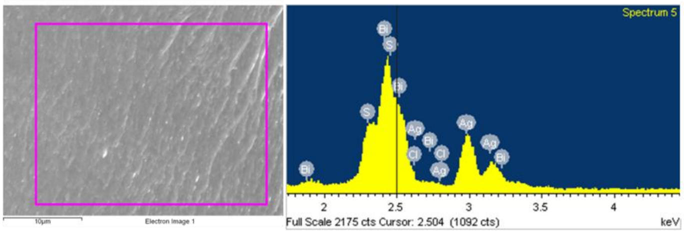

Element	Weight%	Atomic%
S K	6.99	23.95
Cl K	0.37	1.15
Se L	15.47	21.52
Ag L	26.00	26.48
Bi M	51.17	26.90
Totals	100.00	

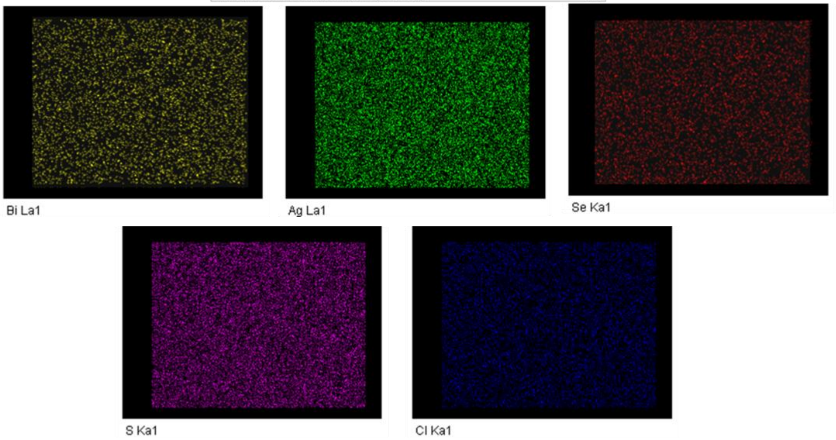

$BiAgSeS_{0.96}Cl_{0.04}$

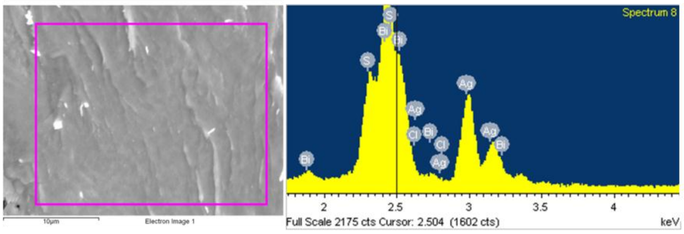

Element	Weight%	Atomic%
S K	7.30	24.37
Cl K	0.46	1.39
Se L	16.88	22.89
Ag L	26.51	26.31
Bi M	48.86	25.04
Totals	100.00	

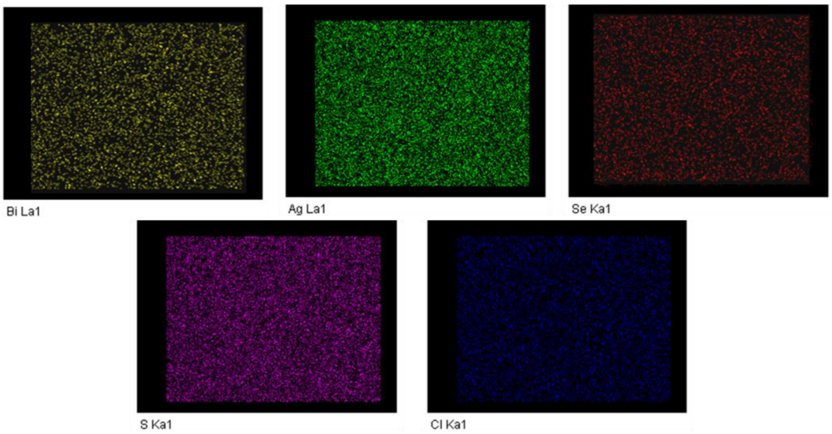

$BiAgSeS_{0.95}Cl_{0.05}$

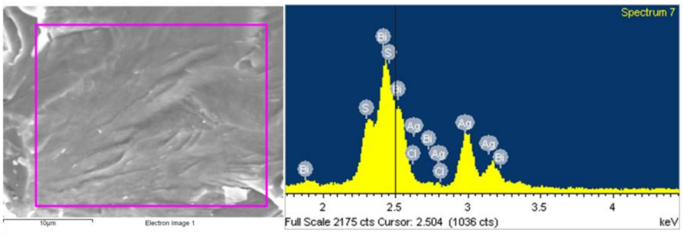

Element	Weight%	Atomic%
S K	7.47	25.10
Cl K	0.52	1.59
Se L	15.61	21.30
Ag L	26.08	26.06
Bi M	50.32	25.95
Totals	100.00	

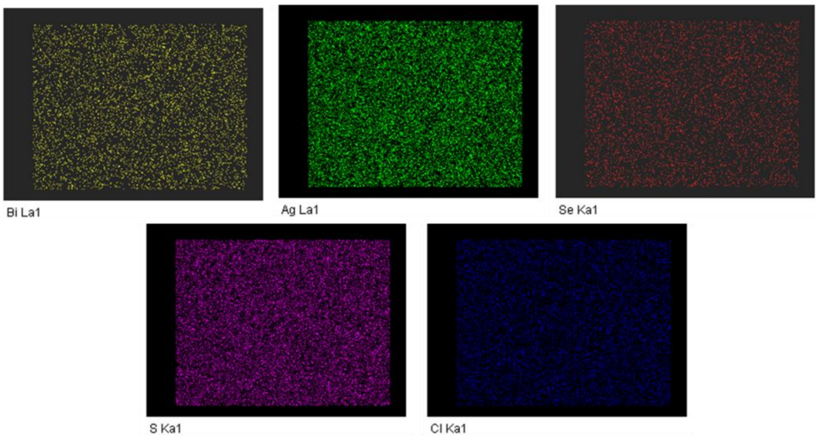

Part 3, supporting figures for properties and characterizations:

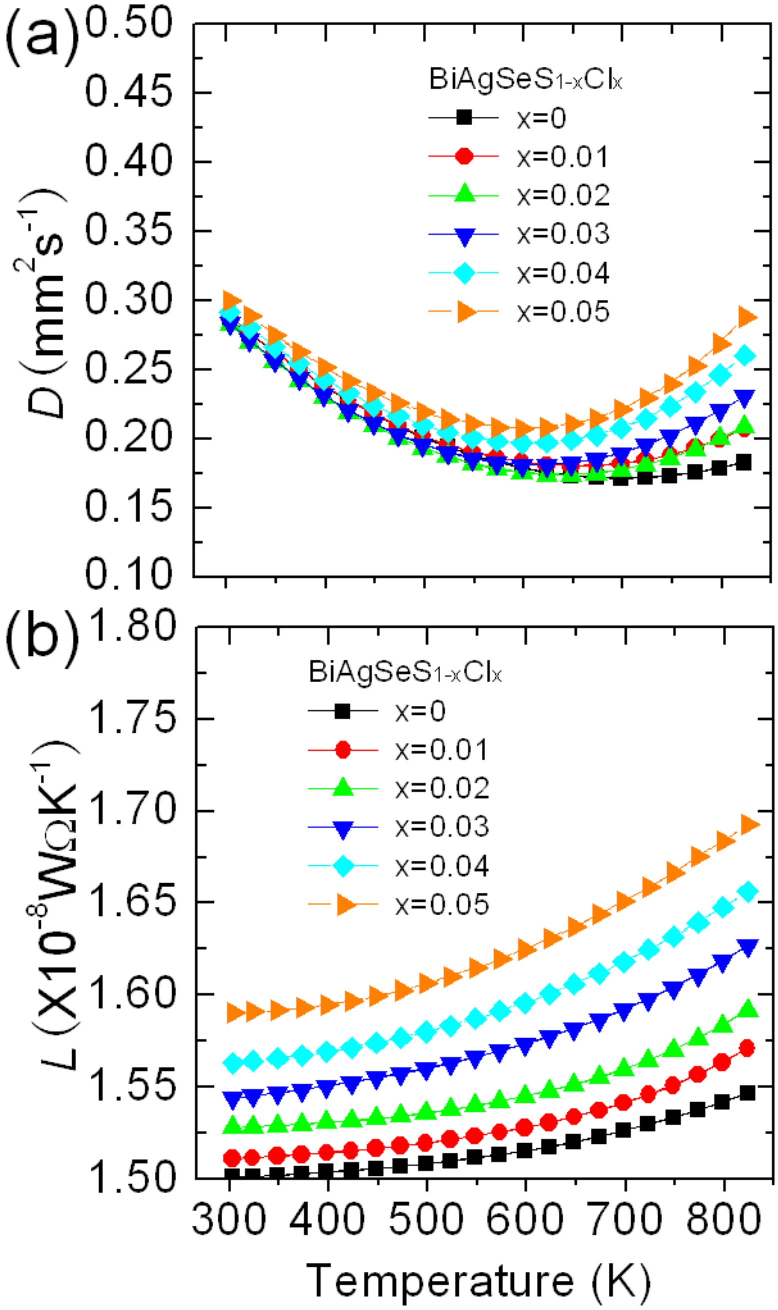

Fig. S1. Thermoelectric properties of BiAgSeS$_{1-x}$Cl$_x$ as a function of temperature: (a) Thermal diffusivity; (b) Lorenz number.

Table S1. Density of samples included in the study.*

Composition	Theoretical Density,[1] g/cc	Measured Density, g/cc	% Theoretical Density
BiAgSeS	7.51	6.765	90.08
$BiAgSeS_{0.99}Cl_{0.01}$	7.51	6.757	89.97
$BiAgSeS_{0.98}Cl_{0.02}$	7.51	6.861	91.36
$BiAgSeS_{0.97}Cl_{0.03}$	7.51	6.731	89.63
$BiAgSeS_{0.96}Cl_{0.04}$	7.51	6.558	87.32
$BiAgSeS_{0.95}Cl_{0.05}$	7.51	6.329	84.27

* Because the Cl alloys completely within the BiAgSeS phases, we do not include Cl doping in the final calculations of density.

[1] A.C. Glatz, A. Pinella, *Journal of Materials Science*, **1968**, *3*, 498-501.

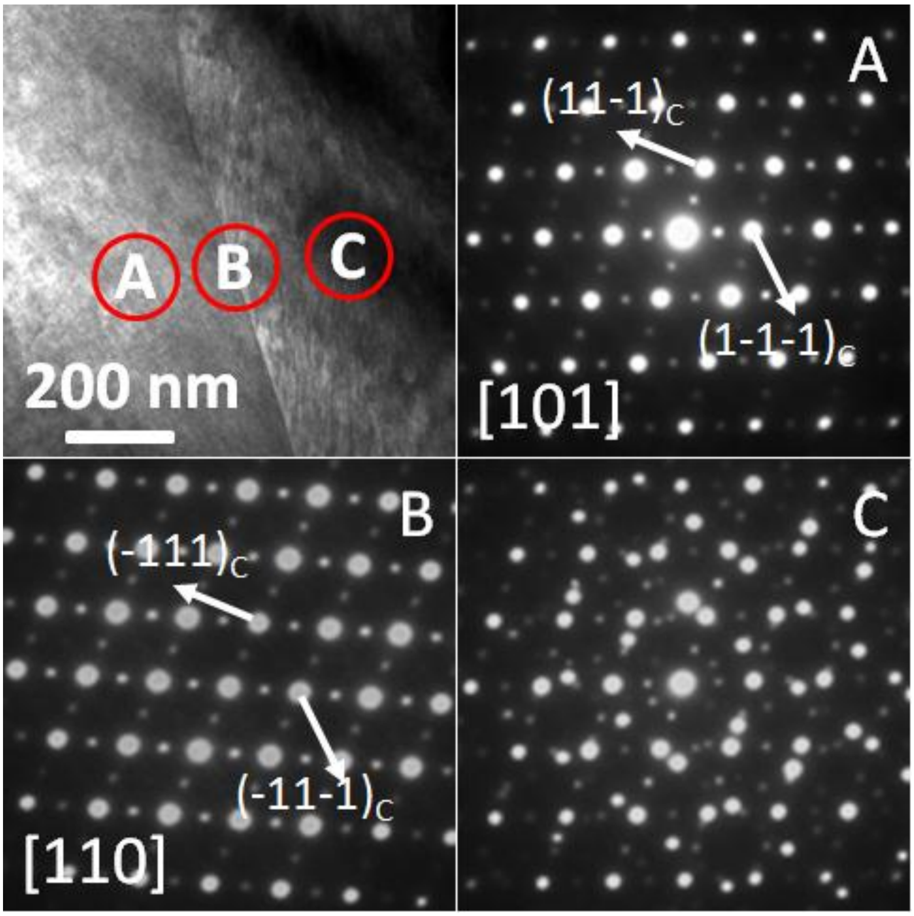

Fig. S2. Low-magnification TEM mage shows a grain boundary and corresponded electron diffraction patterns of area “A”, “B” and “C”, the detailed indexes can be referred to Fig. 4.

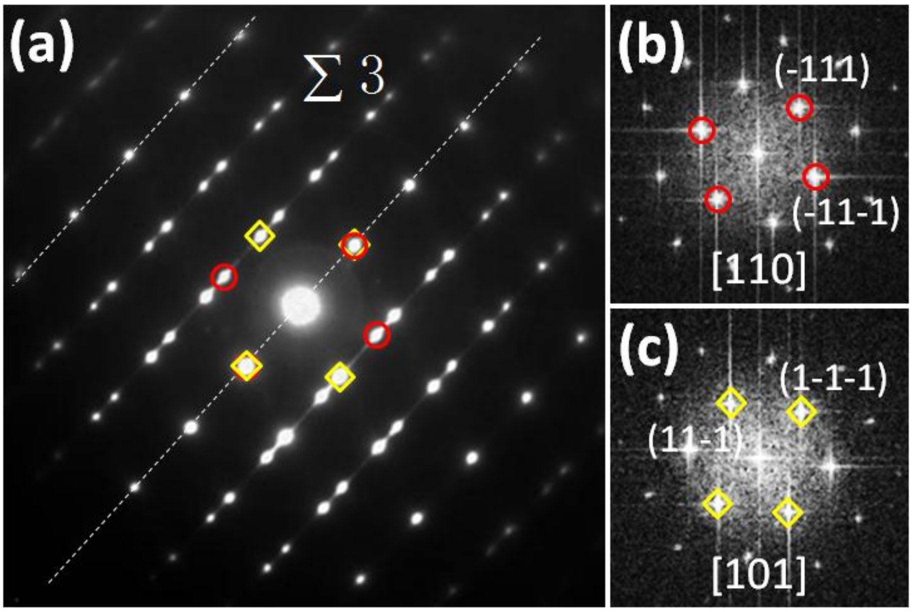

Fig. S3. (a) Electron diffraction pattern of Fig. 3(b). (b) and (c) FFT image of the lower-left and top-right variants respectively.

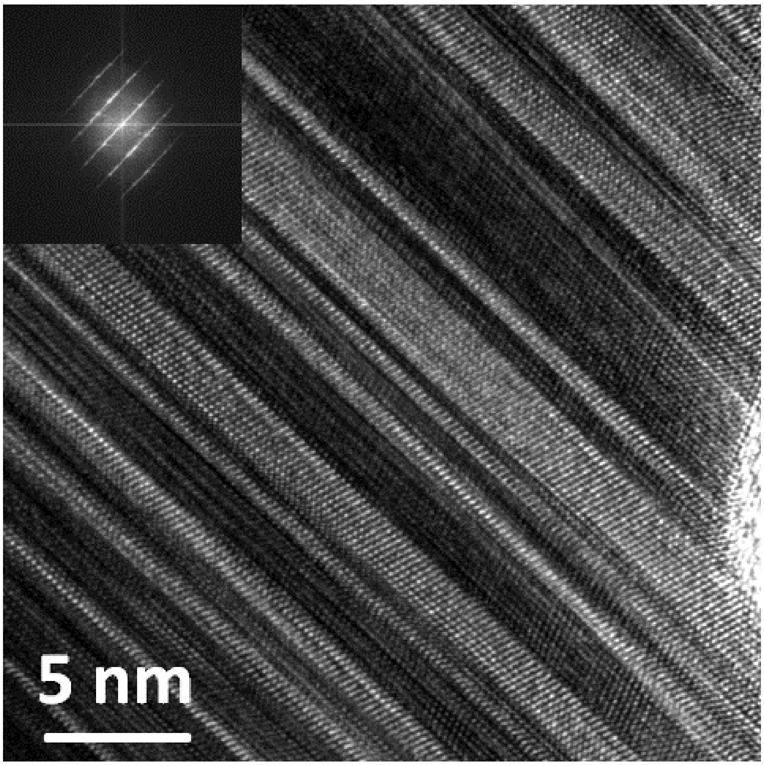

Fig. S4. High-magnification TEM image shows laminated nanostructure with inset FFT image.

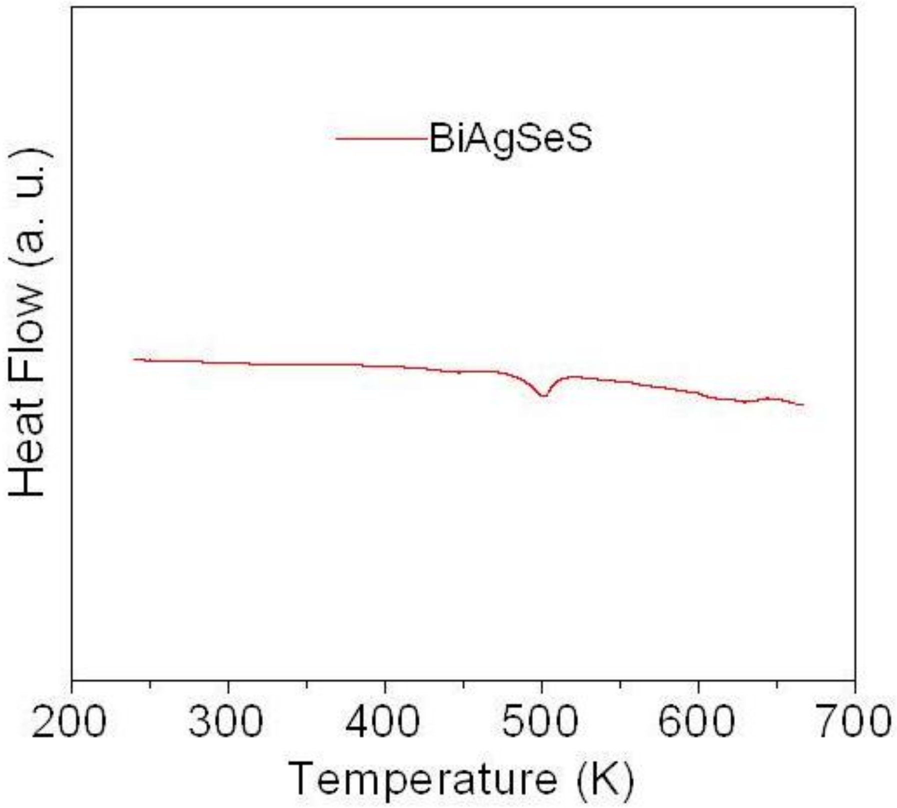

Fig. S5. Differential scanning calorimetry (DSC) for BiAgSeS sample, the presence of an endothermic peak at around 500 K indicates tiny amounts of impurity, which may be related to the laminated precipitates with size range of about 5-15 nm distributes disorderly in the matrix (Figs, 4 (a) and (b)).